QCD PHENOMENOLOGY

Mary K. Gaillard
LAPP, Annecy-le-Vieux, France, and CERN, Geneva, Switzerland

ABSTRACT

Selected topics in QCD phenomenology are reviewed: the development of an effective jet perturbation series with applications to factorization, energy flow analysis and photon physics; implications of non-perturbative phenomena for hard scattering processes and the pseudoscalar mass spectrum; resonance properties as extracted from the combined technologies of perturbative and non-perturbative QCD.

The long-standing, solid prediction of what is now known as "perturbative QCD" is the asymptotic Q^2 dependence of the moments of deep inelastic scattering structure functions. Its formal derivation[1] using the light-cone operator product expansion (OPE)[2] and renormalization group equations (RGE)[3] has now been reformulated[4] in the language of perturbation theory. In addition to making the underlying physics more transparent, this formulation has the advantage that it can be applied to processes for which a light-cone analysis was not appropriate: Drell-Yan dilepton production, semi-inclusive lepton-nucleon and e^+e^- interactions, high p_T phenomena in hadron interactions, jet analyses, and photon interactions. The result is that there is now a basis for treating these processes in terms of a perturbative expansion in the "running" coupling constant $\alpha_s(Q^2)$, where Q^2 is a momentum transfer characteristic of the process studied, a procedure which had, in fact, already been adopted by optimistic phenomenologists[5].

I shall outline the arguments involved in the perturbation theory derivation of the moment equation, indicate how it is extended to other processes, and comment on various phenomenological applications. QCD perturbation theory is known to be inadequate on phenomenological grounds because it cannot account for confinement, and in fact non-perturbative phenomena have been discovered[6] through the study of classical QCD Lagrangians. I shall briefly discuss possible effects of these phenomena on the results of perturbative QCD. However, calculations of non-perturbative phenomena are in their infancy, and results obtained so far can only be considered as indicative. I shall air once again the U(1) problem, which is the issue as to whether the observed pseudoscalar mass spectrum is compatible with QCD, and finally, I shall describe the most ambitious attempt made so far to calculate resonance properties using the full apparatus of perturbative and non-perturbative QCD phenomenology. There are other applications of QCD to hadrons, notably heavy quark decays[7] and the properties of heavy onia[8], which I will not be able to cover. Recent progress in the calculation of electromagnetic form factors[9] will be reported by De Rújula.

1. MOMENTS IN PERTURBATION THEORY

The standard prediction for deep inelastic structure functions takes the form:

$$M_n(Q^2) = \int_0^1 x^n F(x,Q^2)\,dx = M_n(Q_0^2)\left(\frac{\alpha_s(Q^2)}{\alpha_s(Q_0^2)}\right)^{\gamma_n}\left[1+O\left(\frac{1}{\ln Q^2}\right)+O\left(\frac{1}{Q^2}\right)+\cdots\right], \quad (1.1)$$

where x is the usual Bjorken scaling variable;

$$\alpha_s(Q^2) \equiv \frac{12\pi}{33-N_f}\frac{1}{\ln Q^2/\Lambda^2} = g_s^2/4\pi$$

is the strong coupling constant; Q_0 is an arbitrary normalization point conventionally chosen so that $\alpha_s(Q^2) < \alpha_s(Q_0^2) << 1$, and γ_n is a computable number ("anomalous dimension"). The higher-order terms in $(\ln Q^2)^{-1}$ are calculable[10], but the $(Q^2)^{-n}$ terms are partly due to controllable mass effects[11] and partly due to "higher twist" effects which cannot be calculated with present technology. There are two obvious difficulties in confronting (1.1) with the data: experiments are carried out at finite Q^2, and one does not know *a priori* when the Q^{-n} terms will become negligible, and arbitrarily small values of $x = Q^2/2m_p E_{had}$ cannot be attained in finite energy experiments except for small Q^2. Whether or not present data confirm the predictions (1.1) is a controversial issue which will be discussed by de Rújula. We shall assume their validity and sketch their derivation in perturbation theory, so as to display the intuitively plausible features of quark and gluon interactions which may then be generalized to the analysis of other exclusive and semi-inclusive processes.

First recall the OPE-RGE approach, which is based on the observation that the deep inelastic scattering cross-section is related via the optical theorem to the imaginary part of the amplitude for forward Compton scattering of a highly virtual photon (or W, Z) by a proton. The latter amplitude is given by the matrix element between proton states of a time-ordered product of two current operators:

$$\sigma(lN \to l+X) \propto \mathrm{Im}\langle p|T(J_\mu(q), J_\nu(-q)|p\rangle . \tag{1.2}$$

The operator product expansion[2] says that the non-local (q^2-dependent) time-ordered current product can be expressed as a sum of local operators with the q^2 dependence appearing in multiplicative coefficients:

$$T(J_\mu(q), J_\nu(-q)) = \sum O_i(0)\frac{C_i(\ln Q^2)}{Q^{d_i-2}}, \quad Q^2 = -q^2 > 0, \tag{1.3}$$

where d_i is the dimension of O_i in units of mass. The power of Q on the right-hand side is determined by dimensional analysis: the current $J_\mu = \bar{q}\gamma_\mu q$ has dimension three and there is an implicit factor d^4x (d = -4), so the total dimension of the left-hand side is two. For $Q^2 \to \infty$ the dominant term is the one of lowest dimension. (In the Bjorken limit, one takes instead $\nu = p\cdot q \to \infty$, ν/Q^2 fixed; the leading terms in this case have lowest "twist" = dimension minus spin.) The matrix elements $\langle p|O_i|p\rangle$ are unknown, but the Q^2 dependence is contained entirely in the C_i which are determined from the RGE giving the result (1.1) for the leading term.

While this procedure is very formal, the result has nevertheless a simple physical interpretation[12,13]. Once the moments are inverted the deep inelastic cross-section can be expressed as a sum over point-like lepton-parton scattering cross-sections, with, however, Q^2-dependent parton distribution functions:

$$\sigma(\text{"}\gamma\text{"} + N \to X) = \sum_i \int \frac{f_i(x, \ln Q^2)}{x}\sigma(\text{"}\gamma\text{"} + p_i \to X) . \tag{1.4}$$

The influence of quark-gluon interactions is made explicit by the integral equation for the derivative of the distribution functions[13]:

$$\frac{df_i(x,\ln Q^2)}{d\ln Q^2} = \frac{\alpha_s(Q^2)}{2\pi}\int_x^1 \sum_j f_j(y,\ln Q^2)\,T_{ji}\,\frac{dy}{y} \quad . \tag{1.5}$$

The change in the probability of finding parton i at x depends on the probability T_{ji} that it was emitted by parton j at $y > x$ via, for example, gluon bremsstrahlung by a quark (Fig. 1a) or quark pair creation by a gluon. This picture provides an intuitive understanding[12] of the qualitative features of scaling violations. As Q^2 increases, the lepton probe resolves each parton into many partons and "sees" increasingly softer quarks and an increasing anti-quark component. It has also the practical advantage that use of Eq. (1.5) rather than Eq. (1.1) allows a test[14] of the theory without data at small x. However, at this stage, if we forget the formal derivation (1.1)-(1.3), we are still speaking a parton language: the Q^2 dependence of α_s is put in by hand and transverse momentum is neglected.

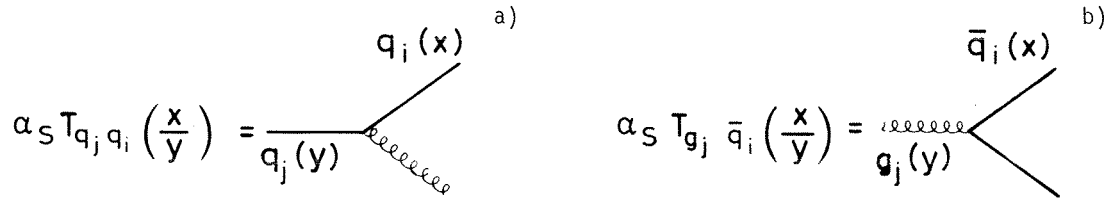

Fig. 1 Primary mechanisms for the Q^2 evolution of structure functions: a) momentum softening via gluon bremsstrahlung and b) sea enhancement via quark pair creation.

Next we turn to perturbation theory[15]. QCD, a theory of quarks interacting with massless vector gluons, has many similarities with QED, the theory of leptons interacting with massless vector photons. Notably we encounter certain infinities in evaluating amplitudes: a) "infrared" singularities; the divergence associated with soft-gluon emission (Fig. 2a) is cancelled by divergences arising from virtual gluon corrections (Fig. 2b); b) "mass" singularities occur when a quark emits a collinear gluon because the quark can remain on mass shell. If k_T is the transverse momentum of the gluon, the bremsstrahlung amplitude is

$$dk_T^2\,\frac{\alpha_s(k_T^2)}{k_T^2} \propto \frac{dk_T^2}{k_T^2 \ln k_T^2} = d(\ln\ln k_T^2)\,, \tag{1.6}$$

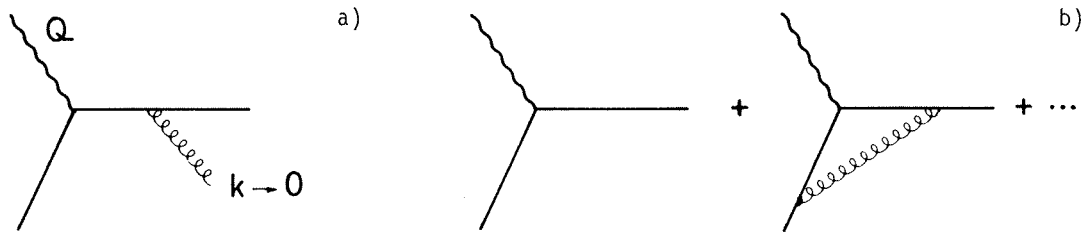

Fig. 2 Diagrams which combine to cancel infrared divergences: a) soft gluon bremsstrahlung and b) virtual gluon corrections.

where the use of the running coupling constant in Eq. (1.6) takes into account virtual gluon radiative corrections. Mass singularities vanish in the sum over collinear configurations of fixed total energy which are physically indistinguishable. Now consider a contribution to deep inelastic scattering illustrated in Fig. 3. Because the gluon bremsstrahlung spectrum diverges for small transverse momentum [Eq. (1.6)], the favoured configuration has all k_T^2 and q_T^2 small and ordered:

$$k_{1T}^2 > k_{2T}^2 > \cdots > k_{nT}^2 \; ; \; q_{1T}^2 > q_{2T}^2 > \cdots > q_{3T}^2 \; . \tag{1.7}$$

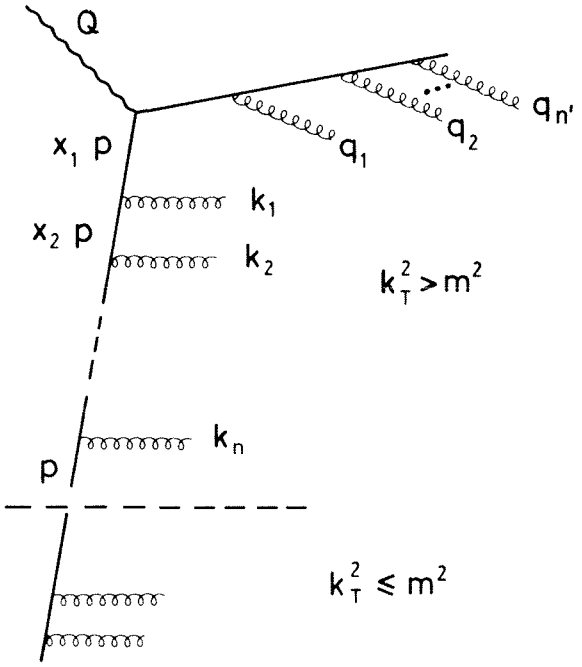

Fig. 3 Multigluon bremsstrahlung contribution to deep inelastic scattering

For inclusive final states, the sum over final-state configurations eliminates mass singularities arising from small q_{iT}. For the incoming quark line, we have to integrate over all the k_{iT}^2. Because of the form (1.6) for the bremsstrahlung spectrum, this integration takes a particularly simple form:

$$\int_0^{\ln\ln Q^2} dz_1 \int_0^{z_1} dz_2 \cdots \int_0^{z_{n-1}} dz_n = \frac{1}{n!}(\ln\ln Q^2)^n + \cdots \; . \tag{1.8}$$

Next we perform the x integration; since the dominant contribution comes from small k_T^2 we can neglect the transverse momenta of the quark lines. Since the scattering is from a quark of fractional momentum x_1, it plays the role of the Bjorken scaling variable and we get

$$\int_0^1 dx_1 \, \delta(1 - x/x_1) \int_{x_1}^1 dx_2 \, T(x_1/x_2) \cdots \int_{x_{n-1}}^1 dx_n \, T\left(\frac{x_{n-1}}{x_n}\right) T(x_n) \; , \tag{1.9}$$

where $\alpha_s T(x/y)$ is the amplitude of Fig. 1a. The folded integrals of formula (1.9) can be unfolded by taking moments; integrating (1.9) over x weighted with x^m gives

$$\int_0^1 dx \, x^m \, [(1.9)] = (T_m)^n \; ; \quad T_m = \int_0^1 dx \, x^{m+1} \, T(x) \; . \tag{1.10}$$

The moments of the structure functions are obtained by summing over n; the result is an exponential

$$M_m \propto \sum_n \frac{1}{n!} \left(T_m \ln\ln Q^2\right)^n = e^{T_m \ln\ln Q^2} = (\ln Q^2)^{T_m} \; , \tag{1.11}$$

which is the same as Eq. (1.1) with $T_m = -\gamma_m$. Actually, the procedure used, which incorporates virtual gluon radiative corrections by the replacement $\alpha_s \to \alpha_s(k_T^2)$ at each vertex, is a valid procedure as long as k_T^2 is large enough so that each quark line is sufficiently off-shell to be insensitive to bound-state effects. For this reason the chain in Fig. 3 has been divided into a subchain with $k_T^2 > m^2 = O(\text{GeV})$, to which the integration and summation procedure described above is applied, and a subchain with $k_T^2 < m^2$, which is left unspecified but which does not govern the Q^2 dependence.

Note that

a) Taking the derivative of Eq. (1.11) we get

$$\frac{dM_m}{d\ln Q^2} \propto \frac{1}{\ln Q^2} T_m M_m \propto \alpha_s(Q^2) T_m M_m \,, \tag{1.12}$$

which is obtained from the Altarelli-Parisi equation (1.5) by taking the m^{th} moment.

b) The result (1.11) corresponds to the "leading log approximation". For example, we neglected the lower end of the integrations ($z_i > \ln \ln m^2$) in Eq. (1.8) and the transverse quark momentum.

c) The perturbation theory result can easily be reinterpreted in terms of the operator product expansion. The squared amplitude corresponding to Fig. 3 is the imaginary part of the "ladder" contribution to Compton scattering (Fig. 4), which by definition has only large momenta $|k^2| > m^2$ running across its rungs. Once the momentum integrations are performed, one gets an effectively local biquark operator with a Q^2-dependent coefficient. Adding on the "soft" rungs at the bottom part of the chain of Fig. 3 corresponds to taking the matrix element between hadron states.

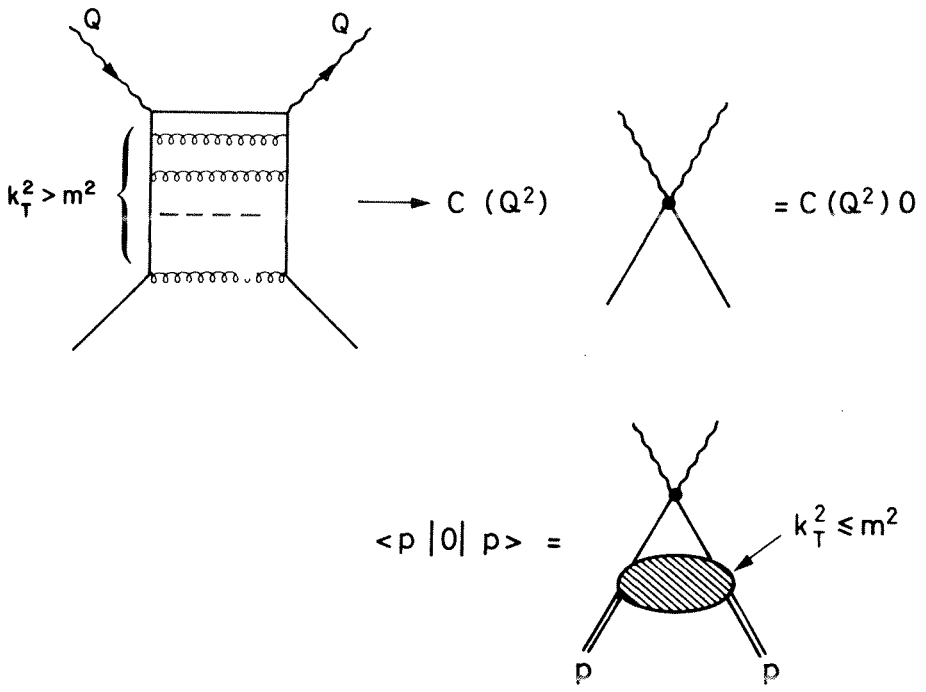

Fig. 4 Operator interpretation of the contribution of Fig. 3

2. FACTORIZATION AND JETS

We saw that the favoured configuration for a hard scattering process is one in which bremsstrahlung gluons are all nearly collinear with an incoming or outgoing quark line. This corresponds to a two-jet configuration. The first subdominant configuration is one in which one high p_T gluon is emitted. This forces a quark far off-mass-shell, and one power of $\ln Q^2$ is lost; the amplitude is then

$$\alpha_s^n (\ln Q^2)^{n-1} = O(\alpha_s(Q^2)) . \tag{2.1}$$

In this order we have to have either k_{1T} or q_{1T} large with $k_{i>1}$, $q_{i>1}$ again all nearly collinear. If large transverse momentum is emitted further down the chain, all the quarks above it are forced off-shell so that more powers of $\ln Q^2$ are lost. The hard gluon (as well as soft ones) is of course also dressed with collinear fragments, and one gets a three-jet configuration as illustrated in Fig. 5. What we see emerging is an effective perturbation series in $\alpha_s(Q^2)$.

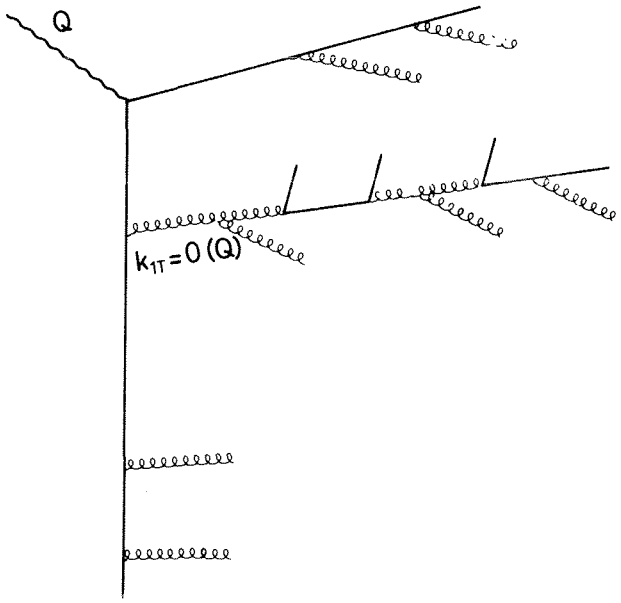

Fig. 5 A leading subdominant contribution to deep inelastic scattering or e^+e^- annihilation giving a three-jet final state

For example, to zeroth order in $\alpha_s(Q^2)$ e^+e^- → two jets via a quasi-collinear configuration analogous to Fig. 3; in order $\alpha_s(Q^2)$ we get the three-jet configuration of Fig. 5, and so forth. In addition, for a process involving a hadronic target or trigger particle, the soft piece ($k_T^2 \leq m^2$) at the bottom of the chain is independent of the number of hard transverse gluons emitted at the top of the chain. This means that the hadron structure/fragmentation function is a universal factor. For example, if the inclusive deep inelastic scattering cross-section is

$$\sigma(\text{"}\gamma\text{"} + N \to X) = \frac{1}{x} f_q(x, Q^2)\, \sigma(\text{"}\gamma\text{"} + q \to q) + \cdots , \tag{2.2}$$

the cross-section for the leading subdominant process with an extra-high p_T jet is given by

$$\sigma(\text{"}\gamma\text{"} + N \to 2 \text{ high } p_\perp \text{ jets}) = \frac{1}{x} f_q(x,Q^2)\,\sigma(\text{"}\gamma\text{"} + q \to q + g) + \cdots, \qquad (2.3)$$

where the cross-section on the right-hand side is to be calculated to lowest order in perturbation theory using the effective quark-gluon coupling constant $\alpha_s(p_T^2)$.

This result is known as "factorization" in the sense that the unknown function which incorporates the bound-state properties is independent of the number of high p_T jets observed in the final state. A more general definition of factorization arises in the description of a process involving more than one target, projectile, or trigger hadron. Factorization was first studied in the lowest non-trivial order in perturbation theory[16]. A quark structure function is determined in perturbation theory by writing the cross-section for deep inelastic lepton-quark scattering in the usual parton language:

$$\sigma(\text{"}\gamma\text{"} + q \to X) \equiv \sum_i \frac{1}{x} f_{i/q}(x,Q^2)\,\sigma(\text{"}\gamma\text{"} + i \to i), \qquad (2.4)$$

where $\sigma(\gamma + i \to i)$ is the point-like cross-section (e.g. Fig. 6a) for scattering from a parton i, and $f_{i/q}(x,Q^2)$ is by definition the distribution function for finding a parton i in a quark. The total cross-section can be calculated in perturbation theory via diagrams such as those in Fig. 6. Next, one calculates the cross-section for the production of Drell-Yan massive lepton pairs in quark-quark scattering via diagrams such as that of Fig. 7, and one finds that the result can be expressed in the form

$$\sigma(qq \to \mu^+\mu^- + X) = \sum_i \frac{1}{x_1 x_2} f_{i/q}(x_1)\, f_{\bar{i}/q}(x_2)\left[\sigma(i + \bar{i} \to \mu^+\mu^-) + O\left(\frac{1}{\ln Q^2}\right) + \cdots\right] + O\left(\frac{1}{Q^2}\right), \qquad (2.5)$$

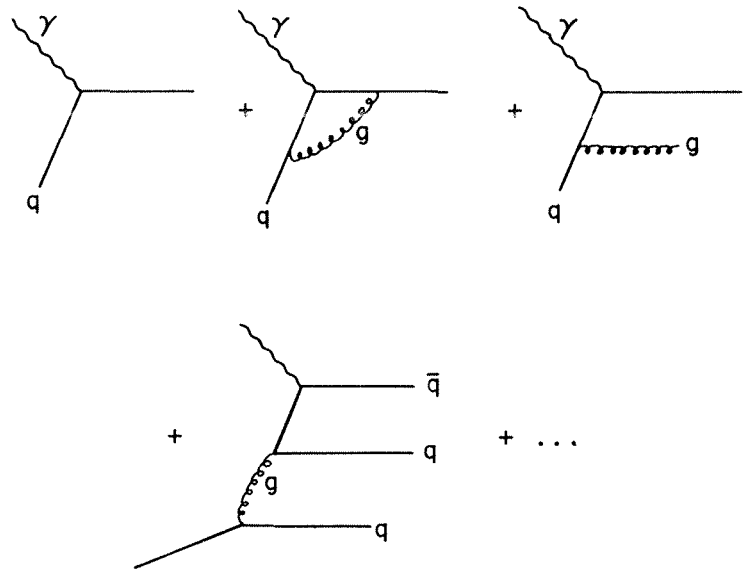

Fig. 6 Diagrams for deep inelastic lepton-quark scattering

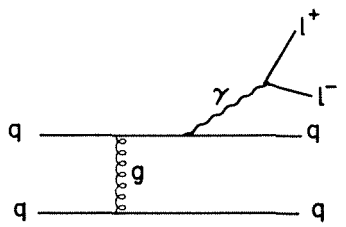

Fig. 7 Diagram contributing to the production of Drell-Yan lepton pairs by quarks

where $f_{i/q}$ and $f_{\bar{i}/q}$ are the quantities extracted from the calculation of (2.4), and $\sigma(i + \bar{i} \to \mu^+\mu^-)$ is the point-like parton-antiparton annihilation cross-section. The structure functions in fact contain mass singularities

$$f_{q/q} = \delta(x-1) + C\alpha_s(Q^2)\ln(Q^2/\mu^2) + \cdots , \tag{2.6}$$

but these are absorbed in a universal factor, which means that [to $O(1/Q^2)$] the Drell-Yan cross-section is calculable in terms of the deep inelastic scattering cross-section. Keeping just the first term in brackets in (2.5) gives just the usual Drell-Yan formula; the $O(1/\ln Q^2)$ terms can also be calculated, and a large amount of work has gone into their study and comparison with data[17].

Analogously, the fragmentation functions for partons into quarks can be defined by calculating perturbatively the cross-section for "one-quark inclusive" e^+e^- annihilation (Fig. 8), and relating it to the fragmentation functions via the formula

$$\sigma(e^+e^- \to q + X) = \sum_i \sigma(e^+e^- \to i + \bar{i})\, D_{q/i}(z) . \tag{2.7}$$

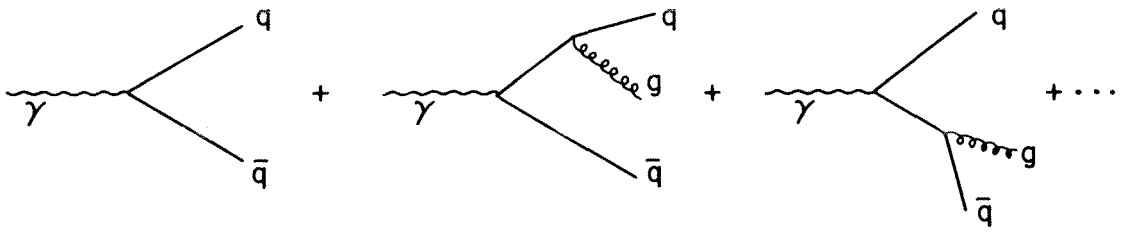

Fig. 8 Diagrams for $e^+e^- \to q + X$

Then a calculation of the two-quark inclusive cross-section shows that it can be expressed as

$$\sigma(e^+e^- \to q + q' + X) = \sum_i \sigma(e^+e^- \to i\bar{i})\left[D_{q/i}(z)D_{q'/\bar{i}}(z') + O(\ln^{-1}Q^2)\right] . \tag{2.8}$$

Similarly, the semi-inclusive deep inelastic cross-section contains as factors the quark structure and fragmentation functions:

$$\sigma(\text{"}\gamma\text{"} + q \to q' + X) = \frac{1}{x}\sum_{i,j} f_{i/q}(x)\, D_{q'/j}(z)\left[\sigma(\text{"}\gamma\text{"} + i \to j) + O(\ln^{-1}Q^2\right] , \tag{2.9}$$

where "γ" is a virtual photon, a $W^{\pm}$, or a Z^0, and high p_T hadron production in hadron collisions contains three "soft" factors:

$$\sigma(q + q' \to q''(p_\perp) + X) = \sum \frac{1}{xx'} f_{i/q}(x)\, f_{j/q'}(x')\, D_{q''/k}(z)\left[\sigma(i + j \to k(p_\perp/z) + X) + O(\ln^{-1}p_\perp^2)\right] , \tag{2.10}$$

where the cross-section on the right-hand side is calculated to lowest order in the running coupling constant $\alpha_s(p_T^2)$.

The results (2.5) to (2.10) have been shown[4,18] to be correct when leading logs are summed to all orders, with the infrared finite $O(\ln^{-1} Q^2)$ or equivalently $O[\alpha_s(Q^2)]$ corrections determined by the next-to-leading logs, analogous to Fig. 5, and so on. However, the results have been demonstrated only for quarks and gluons as target, projectile, and trigger particles, since perturbation theory cannot probe the bound-state properties of the theory. The hope is that the soft blobs at the end of the ladders remain Q^2-independent and factorizable in the presence of non-perturbative effects which are necessarily present. We shall comment later on this point.

3. ENERGY FLOW ANALYSIS

Since the properties of hadrons are not amenable to study in perturbative QCD alone, one would like to find tests of the theory which are independent of these properties. This is the principal motivation behind the various tests of energy flow patterns in e^+e^- annihilation which have recently been proposed. We saw that QCD perturbation theory justifies a perturbative expansion in the effective coupling constant. In e^+e^- annihilation the dominant configuration is two-jet-like, as in Fig. 3; the first subdominant configuration contains three jets, all with large relative $p_T = O(Q)$, and can be calculated from the simple quark-gluon bremsstrahlung amplitude using as coupling constant $\alpha_s(p_T^2) = \alpha_s(Q^2)[1 + O(\ln^{-1} Q^2)]$. On the other hand, for a 1^{--} $q\bar{q}$ resonance, the dominant contribution is a three-jet configuration $(\bar{q}q)_{1^-} \to 3$ gluons.

Just as the observation of a $(1 + \cos^2\theta)$ distribution for two-jet events, characteristic of the production of point-like spin-$\frac{1}{2}$ particles, gave strong support to the physical reality of quarks, we hope that various angular correlations which can be measured in three-jet events on and off resonance will show the patterns expected for spin-one gluons. When multijet events show up with clearly separated jets, their properties can be directly studied in terms of the energies and angles of separate jets. I think that few theorists expected to be seeing so soon such beautiful three-jet candidates as were shown during the talks of Söding and Wolf. At lower energies, for example at the Υ mass, three-jet structures are not visible to the eye, and a number of analyses have been proposed for extracting the hypothesized underlying jet structure and measuring the spin of the gluon. These tests are all based on the principle of avoiding infrared and mass singularities by summing over states which are physically indistinguishable in a theory of quarks and massless gluons. The same criteria also minimize sensitivity to our ignorance of the mechanism by which quarks and gluons are forced to "hadronize" to form the final state which is actually observed.

As a first example, consider the Sterman-Weinberg quantity which measures the fraction of energy flow through a cone of finite angle. For example, one can calculate perturbatively[19,20] the probability that a fraction ε of the total energy in e^+e^- annihilation lies outside a region defined by two back-to-back cones of half-angle δ. This quantity diverges if ε or δ is made arbitrarily small:

$$\frac{\sigma(\varepsilon,\delta)}{\sigma} \underset{\varepsilon,\delta\to 0}{\propto} \frac{\alpha_s}{\pi} \ln\varepsilon \ln\delta + O(\alpha_s^2). \tag{3.1}$$

This divergence reflects the fact that for small ε and δ, one is approaching a perfect two-jet configuration which is sensitive to quasi-collinear or soft multigluon emission, and the perturbation series no longer converges. So in order for such a test to be useful, one has to choose ε, δ sufficiently large:

$$|\ln\varepsilon \ln\delta| << \frac{\pi}{\alpha_s(Q^2)} \quad . \tag{3.2}$$

In addition, we know that jets have an intrinsic p_T spread, presumably governed by hadronization effects which cannot be calculated perturbatively, but which are hopefully Q^2-independent. In order for these effects to contribute negligibly to the measured energy fraction outside a biconical region, we also have to choose

$$\varepsilon, \delta >> \varepsilon_{had}, \delta_{had} \sim \frac{\langle p_\perp^2 \rangle_{had}}{Q^2} \tag{3.3}$$

where $\langle p_T \rangle_{had}$ can at present only be determined experimentally. That the criterion (3.3) is still difficult to satisfy at energies as high as 10 GeV can be seen from Fig. 9, where the average energy flow as a function of the angle δ, measured at 9.4 GeV, is compared with the QCD calculation[21]. Nevertheless, such tests should become feasible at higher energies since the hadronization effects should fall like Q^{-2}, while the perturbative contribution drops only logarithmically. Figure 10 shows[20] the probability, analogous to (3.1), for fractional energy flow outside the principal jet cones in deep inelastic scattering at two values of Q^2; the predictions are nearly indistinguishable. In addition, one can hope to improve comparison between theory and data by a re-summation of the perturbation expansion so as to account for the dominant contribution from multigluon soft/collinear bremsstrahlung, as will be discussed by De Rújula. Since many of the hadronization effects are kinematic in that finite values of

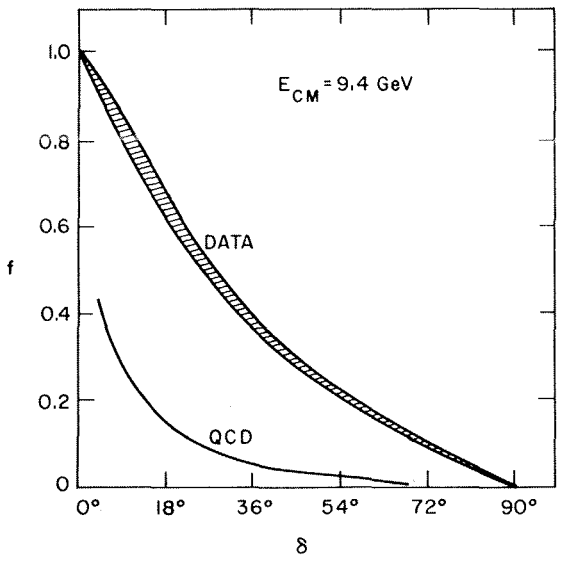

Fig. 9 Comparison[21] of data with QCD prediction for the average energy fraction outside a cone of half-angle δ

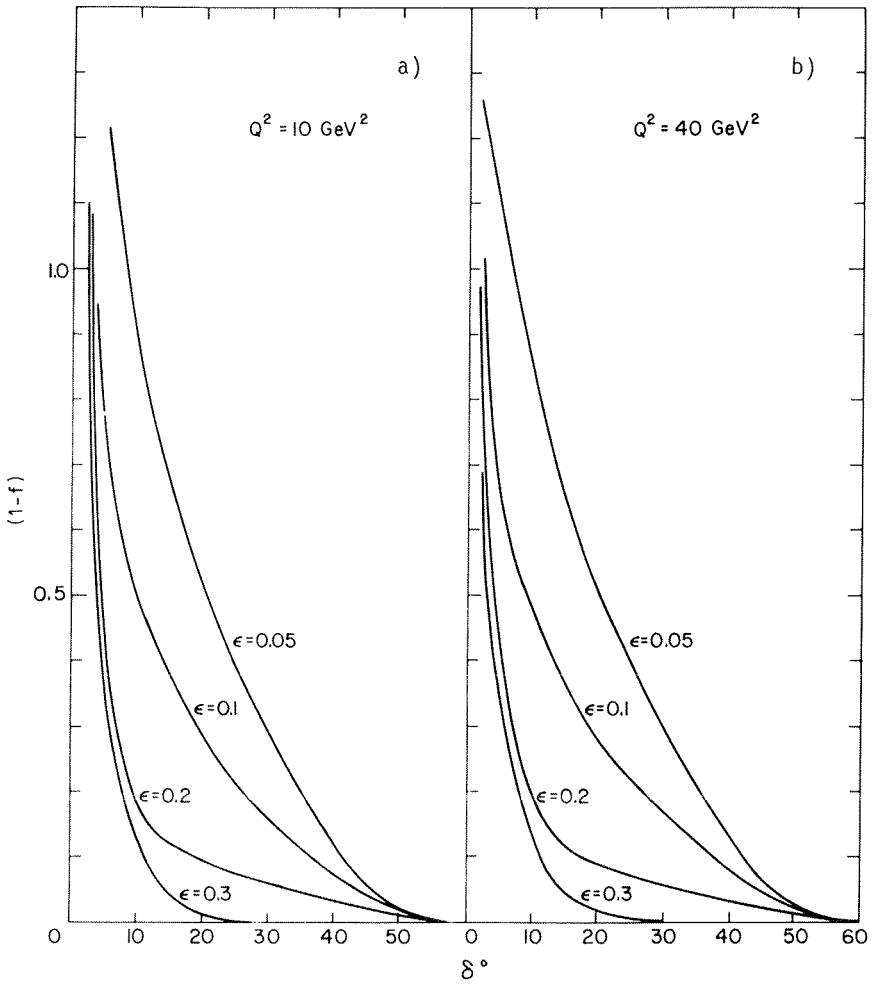

Fig. 10 The calculated probability[20] 1-f that a fraction ε of the energy in the hadronic final-state rest frame in deep inelastic scattering will lie outside back-to-back cones of half-angle δ

$\langle\varepsilon\rangle$, $\langle\delta\rangle$, etc., are directly related to the final-state multiplicity, a re-summation which incorporates multiquanta final state will more closely resemble the true multihadron final state. Of course no improvement of the perturbation series will be able to reproduce the final confining stage of hadronization.

The Sterman-Weinberg procedure tests only the perturbatively induced deviations from ideal two-jet events. There are many other observables which can be calculated perturbatively and which are more specific to the search for gluon jets. The most popular energy flow variables are thrust[22] (T), which measures the sum of parallel energies with respect to the axis which maximizes the parallel energy in one hemisphere of the event sphere; spherocity (S)[23], which measures the sum of transverse energies with respect to the axis which minimizes that quantity; and sphericity ($\hat{S}$)[24], which differs from spherocity in that it measures the sum of energies squared. Thrust and spherocity are "good" variables in that they are indistinguishable for physically indistinguishable collinear configurations, and therefore free of infrared singularities and insensitive to the details of hadronization in the limit of vanishing $\langle p_T \rangle_{had}$. Sphericity does not enjoy these properties, but is apparently[25,26] better

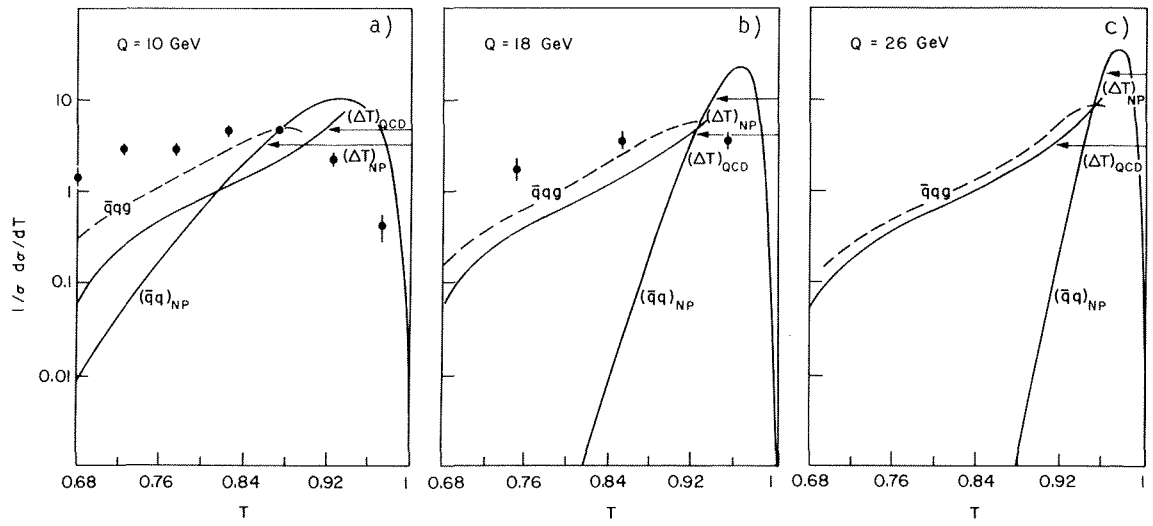

Fig. 11 Thrust distribution[27] for e^+e^- → hadrons at three centre-of-mass energies in order α_s in perturbative QCD. The solid (dashed) lines $q\bar{q}g$ show hard gluon bremsstrahlung without (with) hadronization, and are to be compared with a two-jet model $(q\bar{q})_{NP}$ and the data[28] at 9.4 and 17 GeV (resolution smearing not unfolded).

suited to data analysis than is spherocity. Thrust seems to enjoy the approval of both theorists and experimentalists. In Fig. 11 we show predicted thrust distributions[27] for e^+e^- → hadrons at three energies. The curves marked $(\bar{q}q)_{NP}$ represent a simple model for hadronized two-jet events; the solid $(\bar{q}qg)$ curves are the calculated gluon bremsstrahlung contributions, and the dashed curves are their hadronized versions. The data points[28] are at 9.4 and 17 GeV. Figure 12 shows[27] thrust distributions on resonance, where $(\bar{q}q)_{NP}$ is an estimate of the contributions from the non-resonant e^+e^- → $\bar{q}q$ background and the indirect decay $\Upsilon \to \gamma \to \bar{q}q$. The solid (ggg) curve is calculated from $\Upsilon \to 3$ gluons, and the dashed

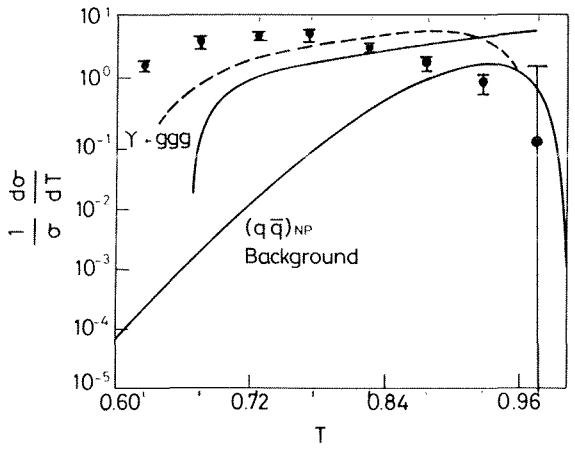

Fig. 12 Thrust distributions[27] on resonance for $\Upsilon \to 3g$ with (dashed) and without (solid) hadronization effects. The two-jet $(q\bar{q})_{NP}$ background is normalized to 1/6 of the three-gluon contribution. The data points[28] are with the two-jet contribution subtracted out (resolution smearing not unfolded).

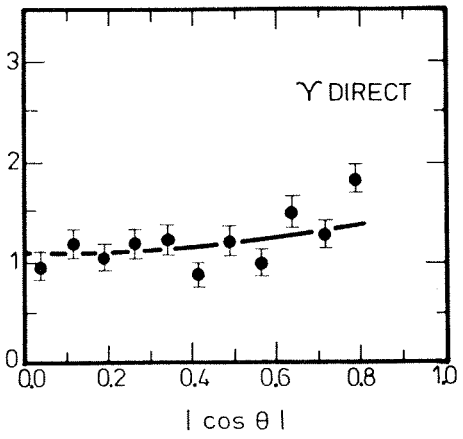

Fig. 13 Measured[29] angular distribution of the sphericity axis and theoretical[30] curve on resonance with the $e^+e^- \to q\bar{q}$ contribution subtracted out

line is hadronized. Figure 13 shows the angular distribution[29] of the thrust axis with respect to the beam direction compared with the prediction[30] for the QCD $\Upsilon \to 3g$ matrix element. The agreement is quite good and the assumption of scalar gluons, for example, cannot reproduce the data.

As discussed by Söding, analysis of the Υ data in terms of the above variables shows consistency with the $\Upsilon \to 3$ gluons hypothesis and a clear deviation from the two-jet-dominated continuum. However, one would like more specific evidence for a three-jet structure of the final state. Analyses of increasing complexity, but still based on "good" (singularity-free) variables, have been proposed. For example, "triplicity"[26] (T_3) is a generalization of thrust which measures the fractional energy parallel to the set of three axes which maximizes this quantity. Triplicity has the property that $T_3 = 1$ for a perfect three-jet event; so measuring both thrust and triplicity allows, in principle, the identification of an event as a three-jet configuration, as illustrated in Table 1. The analysis of the Υ final states in terms of triplicity has been discussed by Söding. Still more sophisticated analyses involve higher moments[31] in the (linearly combined) fractional momenta, up to a full reconstruction[27,32] of the energy flow as a function of the angle in the event plane. Other tests[30,33] exploit the fact that three quanta define three axes in the event plane, and various angular correlations (beam-jet, jet-jet, beam-event plane) can be exploited to test the spins of the final-state quanta.

As discussed by Söding, analyses such as these have been applied to the data in e^+e^- annihilation to look for the three-gluon decay of 1^{--} onia, hard gluon bremsstrahlung in $q\bar{q}$

Table 1
Range of T and T_3 for different event type

Event configuration	Thrust	Triplicity
Two jets	$T = 1$	$T_3 = 1$
Three jets	$\frac{2}{3} < T < 1$	$T_3 = 1$
Multi-jet	$\frac{1}{2} < T < 1$	$3\sqrt{3}/8 < T_3 < 1$
Sphere	$T = \frac{1}{2}$	$T_3 = 3\sqrt{3}/8$

final states in the continuum, and thresholds for new flavour production which are characterized by low thrust and high spherocity. Further applications include the study of cascade onium decays[27,34]. For example, the decays

$$1^{--} \to P + \gamma \quad (\hookrightarrow \text{hadrons}) \,, \tag{3.4}$$

where P is a 0^-, 0^+, or 2^+ state, are predicted to be dominated by a two-gluon hadronic final state. Jet angular correlations with respect to the photon and beam directions are sensitive to the spins of the gluons and of the hadronically decaying state.

Energy flow analysis can also be applied to the final state in hadron-induced reactions. The process[35,36]

$$\ell + N \to \ell' + 3 \text{ jets} \,, \tag{3.5}$$

where two jets have high p_T relative to one another and to the target fragmentation jet, can arise from mechanisms like that of Fig. 5. It is found[36] that contributions to thrust and spherocity distributions have a much higher "hadronization" to "perturbative QCD" ratio than do the corresponding distributions in e^+e^- annihilation, while tests involving angular correlations[36] between the lepton and hadron planes appear to offer more promising tests of the theory. Other applications include[37]

$$pp \to e^+e^- + \text{high } p_\perp \text{ jet} \,, \tag{3.6}$$

arising from the diagrams of Fig. 14, and[38]

$$pp \to \text{high } p_\perp \text{ jets} \,. \tag{3.7}$$

The process (3.7) is potentially very rich, as it involves in lowest order a variety of QCD perturbation theory diagrams (Fig. 15), including the otherwise elusive three-gluon vertex

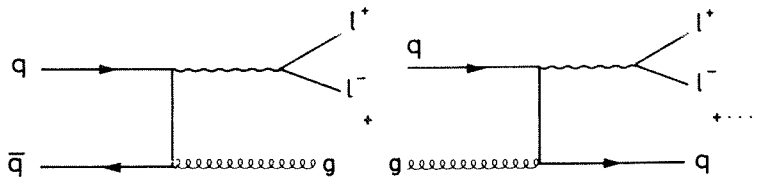

Fig. 14 Contributions to the production of Drell-Yan lepton pairs with large transverse momentum

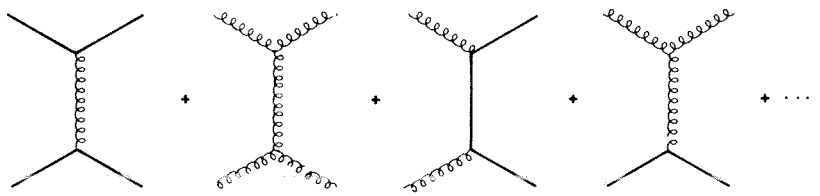

Fig. 15 Contributions to high p_T scattering in hadron collisions

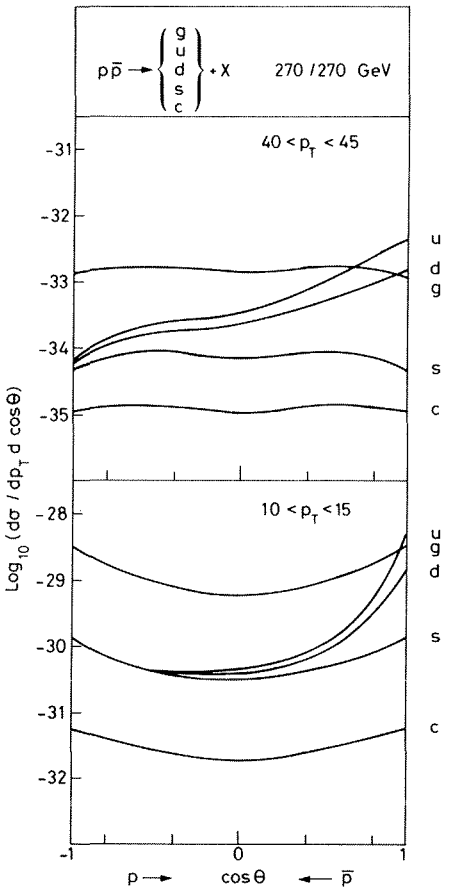

Fig. 16 Calculated[39] angular distributions for jets from different fragmenting quanta in pp̄ collisions at 540 GeV c.m. energy

which is fundamental to the theory. Figure 16 shows a calculation[39] of the angular distributions for jets induced by different types of quanta in pp̄ collisions at 540 GeV centre-of-mass energy. Different quanta arise from different elementary scattering mechanisms, and their relevant importance depends on the parallel momentum of the scattered system, since the initial-state quanta have fractional momentum distributions which depend on their nature. If jet quantum numbers could be identified, these processes would provide detailed tests of the theory. In any case they appear to provide a rich source of gluon jets.

4. PHOTON PHYSICS

As first discussed in terms of the operator product expansion[40], and more recently in the diagrammatic language[41] of perturbation theory, a real or quasi-real photon does not always act like a hadron. To see this[15], consider the deep inelastic scattering of a highly virtual photon from a quasi-real one (Fig. 17). Just as for scattering from a proton, the favoured configuration is for the k_{iT} small and ordered [Eq. (1.7)]. However, because the vertex at the bottom of the chain is point-like, the result of the k_T integration is quite different. Instead of Eq. (1.8) we get

$$\alpha \int^{Q^2} \frac{dk_{1T}^2}{k_{1T}^2 \ln k_{1T}^2} \int^{k_{1T}^2} \frac{dk_{2T}^2}{k_{2T}^2 \ln k_{2T}^2} \cdots \int^{k_{n-2T}^2} \frac{dk_{n-1T}^2}{k_{n-1T}^2 \ln k_{n-1T}^2} \int^{k_{n-1T}^2} \frac{dk_{n-1T}^2}{k_{n-1T}^2} \,. \qquad (4.1)$$

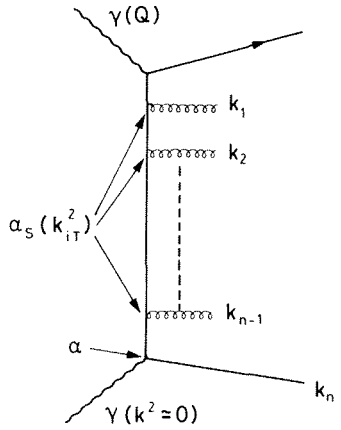

Fig. 17 Multigluon bremsstrahlung contribution to deep inelastic scattering from a photon

The k^2_{nT} integration gives simply $\ln(k^2_{n-1T})$, which cancels the log in the k^2_{n-1T} integration, and so on, giving simply $\alpha \ln Q^2$ for the expression (4.1). The x integration is the same as in Eq. (1.9), except that at the bottom of the chain the $q \to q$ transition function $T(x_n)$ is replaced by a $\gamma \to q$ transition function $T^\gamma(x_n)$. Then taking the m^{th} moment and summing over n gives

$$M^\gamma_m \propto \ln Q^2 \, T^\gamma_m \sum_n (T_m)^n = \frac{\ln Q^2 \, T^\gamma_m}{1 - T_m} \qquad (4.2)$$

instead of Eq. (1.11). The result (4.2) is valid as long as $k_{nT} > m^2$ such that $\alpha_s(m^2)/\pi \ll 1$. In the case where the gluon emission chain continues down to some $k^2_{jT} \lesssim m^2$ before the quark-photon interaction closes the chain, the perturbative treatment has to be stopped at $k^2_{nT} = k^2_{j+1T} > m^2$, giving the result (1.11) with the low k_T contributions absorbed once again into a non-calculable, Q^2-independent distribution function. However, since

$$T_n = -\gamma_n < 0 \quad , \quad \gamma_n > \gamma_{n-1} \qquad (4.3)$$

the higher moments, which govern the high-x region, are suppressed much more strongly with increasing Q^2 in (1.11) than in (4.2), so that for large Q^2 the contribution of (4.2) will be dominant except at very small x. In operator language, the result can be expressed as follows. In addition to the biquark operator of Fig. 4, with coefficient $O(\alpha)$, there is a biphoton operator (Fig. 18) with coefficient $O(\alpha^2)$. But while the matrix element of the biquark operator between photon states is $\alpha \times$ [soft wave function], the matrix element of the biphoton operator is unity. The result[41] for the photon structure function is shown in Fig. 19.

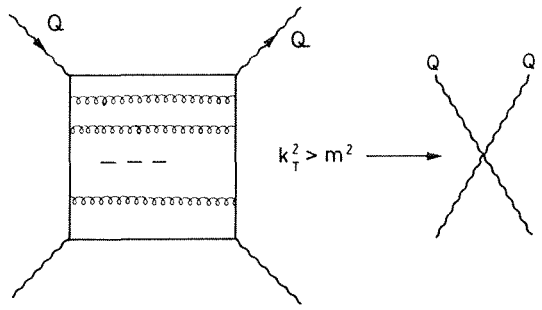

Fig. 18 Operator interpretation of Fig. 17

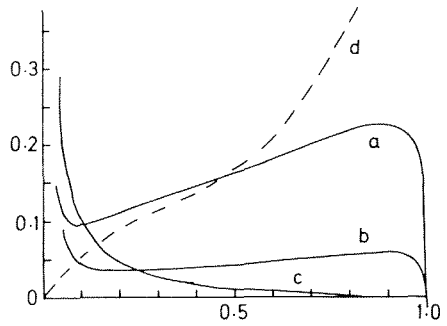

Fig. 19 The functions xq^γ_k and xg^γ in units of $(\alpha/\pi)\ell n Q^2$ [41]: a) xq for $Q_k = \frac{2}{3}$; b) xq for $Q_k = \frac{1}{3}$; c) xg; d) xq for $Q_k = \frac{2}{3}$ in Born approximation (no strong interactions).

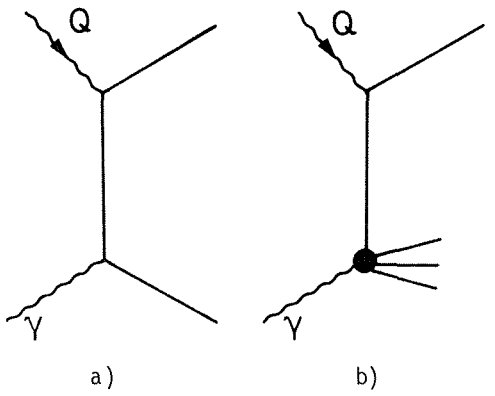

Fig. 20 Two calculable mechanisms for hard processes involving photons: a) point-like photon interaction and b) scattering from a parton

The photon has also a purely point-like contribution to hard scattering processes, so that processes involving real photons and large momentum transfers are dominated by two calculable mechanisms: a QED contribution (Fig. 20a), and a parton scattering contribution (Fig. 20b). These two contributions have different kinematic characteristics which allow them to be distinguished[42,43] experimentally and therefore tested separately. Applications include production of photons[44] with large transverse momentum relative to the jet axis in e^+e^- annihilation, two-photon processes[42,45] in e^+e^- scattering, and production of high p_T photons in photon-hadron scattering[43]. These processes measure the fourth power of the charge of the exchanged quark and so can be used to distinguish Gell-Mann - Zweig charge assignments from those of the Han-Nambu model, for example[46].

5. INSTANTON PHENOMENOLOGY

The study of non-perturbative phenomena in QCD has led to the observation[6,47] that the physical vacuum is a superposition of states $|n\rangle$ with non-trivial gluon field configurations which can be represented by:

$$|\theta\rangle = \sum_n e^{in\theta} |n\rangle \quad , \tag{5.1}$$

where the angular parameter θ which specifies the true vacuum is *a priori* arbitrary. Amplitudes for physical processes can be represented as vacuum-to-vacuum matrix elements of some (non-local) operator O:

$$\langle\theta|O|\theta\rangle = \sum e^{i(n-n')} \langle n|O|n'\rangle = \sum_\nu e^{i\nu\theta} \langle O\rangle_\nu \quad , \tag{5.2}$$

where the equality on the right incorporates the fact that amplitudes involving tunnelling between vacua depend only on the difference $\nu = n-n'$, and ν is the topological quantum number

$$\nu = \frac{\alpha_s}{8\pi} \int d^4x \, \tilde{F}^i_{\mu\nu}(x) F^i_{\mu\nu}(x) \quad , \tag{5.3}$$

where $F^i_{\mu\nu}$ is the gluon field strength tensor and $\tilde{F}^i_{\mu\nu}$ its dual:

$$\tilde{F}^i_{\mu\nu} = \varepsilon_{\mu\nu\rho\sigma} F^{i\rho\sigma} \quad . \tag{5.4}$$

The operator (5.3) is odd under P and CP, so that if $\theta \neq 0$, the amplitude (5.2) violates P and CP as discussed in the talk of Iliopoulos. Here we shall ignore this possibility. All known solutions of the classical gluon field equations are self-dual or anti-self-dual:

$$\tilde{F}^i_{\mu\nu} = \pm F^i_{\mu\nu} \quad . \tag{5.5}$$

The calculation of an amplitude $\langle O \rangle_\nu$ in (5.2) can be represented in a semi-classical approximation as the corresponding Feynman amplitude in the presence of an external field with the property (5.3) and weighted with an exponential damping factor e^{-S}, where S is the classical action:

$$S = \frac{1}{4}\int d^4x\, F^i_{\mu\nu}(x)\, F^i_{\mu\nu}(x) = \pm \frac{2\pi}{\alpha_s}\nu \quad > 0 \tag{5.6}$$

for (anti-)self-dual solutions (5.5). For small α_s, non-perturbative effects are strongly damped for large ν. The case $\nu = 0$ reduces to the usual (zero external field) perturbative treatment, and the largest non-trivial field contribution is the one-(anti-)instanton configuration[6] with $\nu = \pm 1$. This configuration corresponds to an effective external field localized at a space-time point z with space-time extension ρ. In this case α_s in Eq. (5.6) is effectively the running coupling constant defined in Eq. (1.1) with the substitution $Q \to 1/\rho$, so that the effects of small instantons are increasingly suppressed. If processes involving high-momentum transfer are sensitive only to vacuum fluctuations over a space-time extension characteristic of the interaction, $\rho \sim 1/Q$, then retention of only the tunnelling amplitudes of smallest action may represent a good approximation to non-perturbative effects.

The simplest such effect which can be studied is the non-perturbative contribution to $e^+e^- \to$ hadrons[48], which is determined by the imaginary part of the photon vacuum polarization. The one-instanton contribution is illustrated in Fig. 21a with quantum fluctuations (gluon exchange corrections to quark loops) neglected. The calculation differs from the free quark, or parton model, calculation in that the quark propagator has to be evaluated in the presence of an external instanton field[49]. The amplitude is then integrated over the instanton position z and size ρ, weighted by a density function $d(\rho\Lambda, m_q/\Lambda)$. The size integration diverges for large ρ, but the imaginary part is finite and gives a correction to the cross-section ratio

$$R = \frac{\sigma(e^+e^- \to \text{hadrons})}{\sigma(e^+e^- \to \mu^+\mu^-)}, \quad \frac{(\Delta R)_{\text{inst.}}}{R} \simeq \left(\frac{Q}{1\,\text{GeV}}\right)^{-12} (\ln Q^2)^{N_f}, \tag{5.7}$$

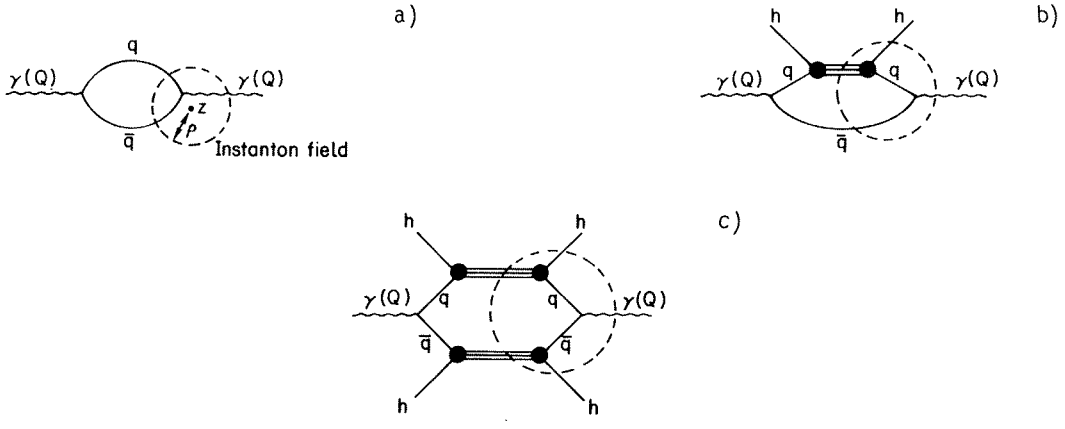

Fig. 21 Diagrams for evaluating instanton effects in a) $e^+e^- \to$ hadrons, b) $\ell + h \to \ell' + X$ or $e^+e^- \to h + X$, c) $h + h' \to \ell^+\ell^- + X$, $\ell + h \to \ell' + h' + X$ or $e^+e^- \to h + h' + X$.

where N_f is the number of quarks with $m_q \lesssim Q$, and conventional estimates of Λ and m_q have been used in determining the scale factor of 1 GeV. For $Q \lesssim 1$ GeV the correction (5.7) is O(1), implying a breakdown of the approximation used, but it becomes rapidly negligible for higher Q^2, suggesting a nice rationale for precocious scaling: the resonance region necessarily involves the non-perturbative aspects of QCD, but immediately above this region we recover the parton model results.

As the next step in complexity we can consider processes involving a hadron as the target or trigger particle, illustrated in Fig. 21b where h can be the target nucleon in deep inelastic scattering or the trigger hadron in one-particle semi-inclusive e^+e^- annihilation. The corrections[50] to the Q^2 dependence again turn out to be $O(Q^{-12})$, but there is a correction O(1) to the normalization. This is again intuitively plausible because the input quark distribution $F(Q_0^2)$ [or fragmentation function $D(Q_0^2)$] is in any case not calculable in perturbative QCD and is expected to reflect the non-perturbative aspects of the theory which determine the properties of hadrons as bound states.

Finally, we can consider the two-hadron semi-inclusive processes illustrated in Fig. 21c, which can represent Drell-Yan lepton pair production, one-particle semi-inclusive deep inelastic scattering, or two-particle semi-inclusive e^+e^- annihilation. In the one-(anti-) instanton approximation these processes fail to exhibit factorization[51]. For example, if Fig. 21b represents inclusive deep inelastic scattering, the resulting cross-section can be parametrized in terms of a structure function $F(x, Q^2)$, but the Drell-Yan cross-section extracted from Fig. 21c does not factorize in terms of the product of structure functions $F(Q^2, x_1)\, F(Q^2, x_2)$. On the other hand, the Q^2 dependence does factorize. If the moments of the structure functions are

$$\int_0^1 dx\, x^n F(x, Q^2) = A_n (\ln Q^2)^{\gamma_n} + O(Q^{-12}) \tag{5.8}$$

the appropriate double moments of the Drell-Yan cross-section take the form

$$\int_0^1 dx_1\, dx_2\, x_1^n x_2^m\, \sigma_{DY}(x_1, x_2, Q^2) \propto A_{nm} (\ln Q^2)^{\gamma_n+\gamma_m} + O(Q^{-12}), \tag{5.9}$$

$$A_{nm} \neq A_n A_m .$$

It is therefore of interest to test independently the factorization of normalization and of the Q^2 dependence in double moments.

As I emphasized before, the calculations done up to now are very rudimentary and should only be taken as indicative. Instanton phenomenology has also been applied to heavy-quark bound state systems[52], but the results depend on a cut-off which has to be imposed on the size integration[53].

6. THE U(1) PROBLEM

The U(1) problem[54] arises from the manifest chiral symmetry of the QCD Lagrangian:

$$\mathcal{L}_{QCD} = \bar{q} M q + \bar{q} \gamma_\mu D_\mu q + F^i_{\mu\nu} F^{i\mu\nu}, \tag{6.1}$$

where M is the quark-mass matrix. One can define vector and axial vector currents

$$V_\mu^\alpha = \bar{q}_\alpha \gamma_\mu q_\alpha \quad , \quad A_\mu^\alpha = \bar{q}_\alpha \gamma_\mu \gamma_5 q_\alpha \quad , \tag{6.2}$$

where α is a flavour index, which are conserved in the limit of vanishing quark mass, $M \to 0$, because in this limit the Lagrangian (6.1) conserves quark helicity. In the real world with finite quark masses, the symmetries associated with vector current conservation are observed to be approximate symmetries of the particle spectrum, while the "chiral" symmetries associated with axial current conservation are not. Chiral symmetry would imply approximately degenerate parity doublets; their absence is attributed to a spontaneous symmetry breaking such that the helicity-violating operators $\bar{q}_\alpha q_\alpha$ acquire (flavour independent) non-vanishing vacuum expectation values $\langle \bar{q}q \rangle \neq 0$. The original symmetry of the Lagrangian manifests itself through the appearance of massless (in the limit $M \to 0$) pseudoscalar particles called Goldstone bosons; the action of an axial charge on a state $|X\rangle$ relates it to the same state plus the appropriate pseudoscalar. For the I = 1 axial current

$$A_\mu^1 = \bar{u} \gamma_\mu \gamma_5 u - \bar{d} \gamma_\mu \gamma_5 d \quad , \tag{6.3}$$

which is conserved for $m_{u,d} = 0$, the Goldstone boson is the nearly massless pion $A|X\rangle \to |\pi X\rangle$. The U(1) problem is the absence of an equally light I = 0 pseudoscalar, since the isoscalar axial current

$$A_\mu^0 = \bar{u} \gamma_\mu \gamma_5 u + \bar{d} \gamma_\mu \gamma_5 d \tag{6.4}$$

is also conserved in the limit $m_{u,d} = 0$.

In fact the last statement is not true in QCD. The "anomalous" triangle diagram of Fig. 22 contributes a non-vanishing term to the divergence of the isoscalar current, while the analogous term for the isovector current cancels between the u- and d-exchange contributions. More generally, for an SU(n) flavour-symmetric current

$$A_\mu^n = \sum_{\alpha=1}^{n} \bar{q}_\alpha \gamma_\mu \gamma_5 q_\alpha \quad , \tag{6.5}$$

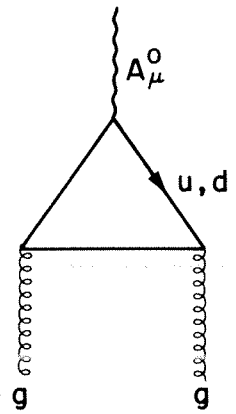

Fig. 22 Anomalous contribution to the isoscalar axial current divergence

the divergence is given by

$$\partial^\mu A^n_\mu = \sum_{\alpha=1}^{n} m_\alpha \bar{q}_\alpha \gamma_5 q_\alpha + \frac{n\alpha_s}{4\pi} \tilde{F}^i_{\mu\nu} F^{i\mu\nu} . \tag{6.6}$$

The last term on the right of Eq. (6.6) can also be written as the divergence of a current

$$K^n_\mu = \frac{n\alpha_s}{4\pi} \varepsilon_{\mu\rho\sigma\tau} A^{i\rho} F^{i\sigma\tau} \tag{6.7}$$

Then we can define a new "partially conserved" current

$$\tilde{A}^n_\mu = A^n_\mu - K^n_\mu ,$$

$$\partial^\mu \tilde{A}^n_\mu = \sum_\alpha m_\alpha \bar{q}_\alpha \gamma_5 q_\alpha , \tag{6.8}$$

and we are apparently back to the same problem. However, the current $\tilde{A}_\mu$ is not invariant under colour gauge transformations, so it has been argued[55] that its matrix elements, like those of quark and gluon fields, are unobservable, and the associated Goldstone boson is effectively confined. More recently, it has been pointed out[56] that non-perturbative effects violate chiral symmetry; the flavour singlet operator $\tilde{F}\cdot F$ which appears in vacuum tunnelling amplitudes [Eq. (5.2)] via the factor $e^{i\theta\nu}$ is a helicity-flip operator since it couples to $\bar{q}\gamma_5 q$ through the gluon-quark coupling.

However, it has been counter-argued[57] that an examination of the Ward identities involving only matrix elements of observable currents shows that the preceding remarks are insufficient to solve the U(1) problem. For example, if $\tilde{A}^n_\mu$ is conserved, one gets the identity

$$\lim_{p\to 0} p_\mu \langle T(\tilde{A}^n_\mu(p), \bar{q}_\alpha \gamma_5 q_\alpha)\rangle = \begin{cases} \langle \bar{q}_\alpha q_\alpha \rangle , & \alpha \le n \\ 0 , & \alpha > n . \end{cases} \tag{6.9}$$

The right-hand side of (6.9) has to be non-zero because of the non-observation of a chiral-symmetric particle spectrum, but the left-hand side can only be non-zero if there is a zero-mass pole giving the contribution illustrated in Fig. 23. This is one formulation of the U(1) problem. If we argue that the matrix element of Fig. 23 is unobservable, we have to consider instead the non-conserved current A_μ.

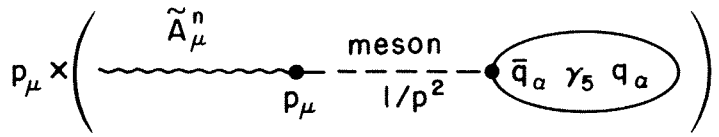

Fig. 23 Pole contribution to the amplitude of Eq. (6.9)

For M = 0 we get the Ward identity

$$\lim_{p\to 0} p_\mu \langle T(A^n_\mu(p), \bar{q}_\alpha \gamma_5 q_\alpha)\rangle = 2n \langle T(\nu, \bar{q}_\alpha \gamma_5 q_\alpha)\rangle + \langle \bar{q}_\alpha q_\alpha \rangle$$

$$= 2ni \frac{\partial}{\partial\theta} \langle \bar{q}_\alpha \gamma_5 q_\alpha \rangle + \langle \bar{q}_\alpha q_\alpha \rangle , \qquad (6.10)$$

where we have used the definition (5.3) and evaluated the amplitude between physical θ-vacuum states, Eq. (5.2). The left-hand side has to vanish since there is no (approximately) zero-mass pseudoscalar which can give a contribution like that of Fig. 23. Then the right-hand side determines the θ-dependence of vacuum expectation values of quark density operators; it can be solved by rewriting it in terms of the combination $\langle \frac{1}{2}\bar{q}_\alpha(1 \pm \gamma_5)q_\alpha\rangle$, giving

$$\langle \bar{q}_\alpha q_\alpha \rangle_\theta = \begin{cases} \cos(\theta/n) \langle \bar{q}_\alpha q_\alpha \rangle_0 & , \alpha \le n \\ \langle \bar{q}_\alpha q_\alpha \rangle_0 & , \alpha > n \end{cases} . \qquad (6.11)$$

This means that in the chiral SU(n) limit, the vacuum expectation values of $\langle\bar{q}q\rangle$ for the n massless quarks are θ-dependent, and furthermore if $\theta \neq 0$ they depend on the number of massless quarks. This is contrary to our customary thinking, according to which $\langle\bar{q}q\rangle$ is approximately flavour-independent and there is a smooth transition between the chiral SU(3) limit, where u, d, and s masses can be neglected, and the still better approximation of chiral SU(2) symmetry, $m_s \neq 0$, $m_{u,d} = 0$.

Is this limit-dependence a problem? Nature has chosen a fixed set of quark masses, and we cannot test experimentally the way amplitudes depend on how the chiral limit is approached. We have to rely on the experts to decide: at the time of writing, Crewther and Coleman are still arguing the issue. Crewther has offered a resolution[57,58] by speculating that the quasi-massless isoscalar Goldstone boson is absent only for isolated values of θ, one of them being the CP and P conserving value θ = 0 which nature has apparently chosen.

An alternative view[59] is that an isoscalar "pseudo-Goldstone boson" does occur, but that very large SU(3) symmetry-breaking effects in $(\bar{q}q)$-(gg) mixing give it a large mass so that it can be identified with the η′.

7. RESONANCE PROPERTIES IN QCD

As the final topic, I shall briefly describe the most ambitious attempt[60] to date to combine results of both perturbative and non-perturbative QCD in a calculation of resonance properties. Just as the deep inelastic scattering cross-section is expressible as the imaginary part of the matrix element of a non-local current-current product between nucleon states [Eq. (1.2)], the cross-section for e^+e^- annihilation into hadrons can be expressed as the matrix element of the same operator between vacuum states (vacuum polarization). However, in order to avoid the *a priori* uncalculable effects of thresholds and resonance structure for time-like Q^2, it is more convenient to relate the cross-section to the vacuum polarization through a dispersion relation; defining

$$\langle T(J_\mu(q), J_\nu(-q))\rangle = (q_\mu q_\nu - q^2 g_{\mu\nu})\Pi(Q^2),$$

$$Q^2 = -q^2 > 0, \qquad (7.1)$$

we can write a subtracted dispersion relation:

$$\Pi' = Q^2 \frac{\partial}{\partial Q^2} \Pi(Q^2) = \frac{Q^2}{\pi} \int_{s_{th}}^{\infty} \frac{\sigma(e^+e^- \to \text{hadrons}, s)\, ds}{(Q^2+s)^2} \quad . \tag{7.2}$$

Using the operator product expansion [Eq. (1.3)] for the current-current product, the left-hand side of (7.2) is expanded according to

$$\Pi' = \sum_i \frac{C_i(\ln Q^2)}{Q^{d_i}} \langle O_i \rangle = C_0(\ln Q^2) + \frac{C_2(\ln Q^2)\, m_q \langle \bar{q} q \rangle}{Q^4}$$

$$+ \frac{C_2'(\ln Q^2) \langle F^i_{\mu\nu} F^{i\mu\nu} \rangle}{Q^4} + O(Q^{-6}) \quad . \tag{7.3}$$

Contributions to the three leading operators in the expansion are shown in Fig. 24. In perturbation theory the vacuum expectation values of quark and gluon density operators vanish, but we know that $\langle \bar{q}q \rangle \neq 0$ because of the chiral asymmetry of the vacuum and $\langle F \cdot F \rangle \neq 0$ because of vacuum tunnelling. In addition, there are the $O(Q^{-12})$ non-perturbative effects discussed in Section 5. These are interpreted as a breakdown of the operator product expansion, which is therefore useful only for Q^2 large enough so that they are negligible. To the extent that the right-hand side of (7.3) can be calculated from theory, and the right-hand side of (7.2) can be evaluated using data, one gets a test of the theory. In particular, the leading term in (7.3) gives the asymptotic-freedom-corrected parton model result which relates R to the sum of squared quark charges.

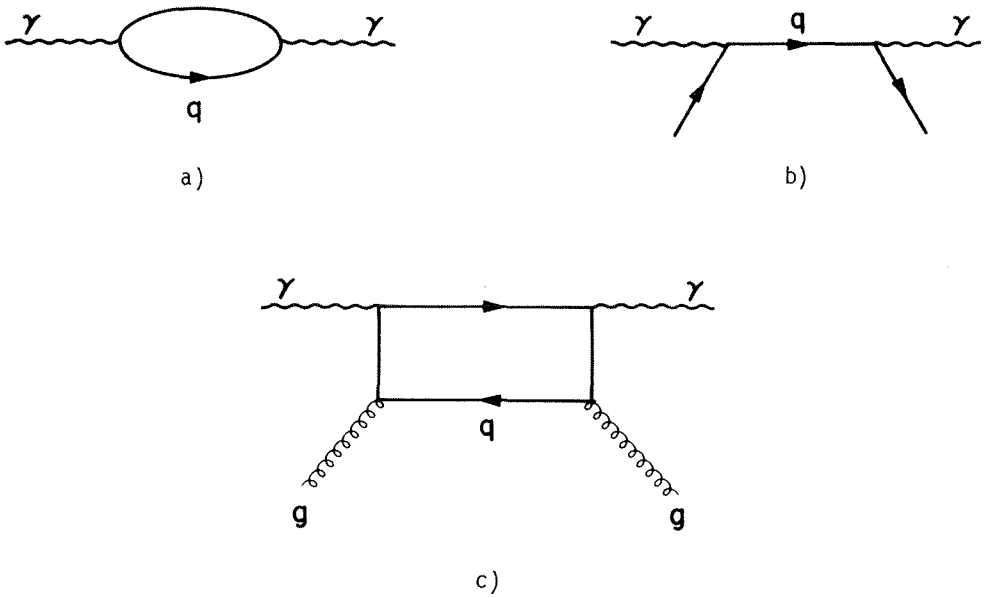

Fig. 24 Diagrams contributing to the leading operators in the current-current product expansion: a) unit operator, b) quark scalar density, c) gluon scalar density.

What one would like to do here is to probe resonance structure by chosing a value $Q^2 \sim 1$ GeV which emphasizes the resonance region of the dispersion integral, but this presents two major problems. For such low values of Q^2, higher-order terms in the expansion remain important, and the integrand in Eq. (7.2) does not converge rapidly enough to damp high Q^2 contributions to the integral. Shifman et al. have improved the situation by considering instead of (7.2) the quantity

$$\lim_{\substack{Q^2,n\to\infty \\ Q^2/n = M^2}} \frac{1}{(n-1)!} Q^{2n}\left(-\frac{d}{dQ^2}\right)^n \Pi \tag{7.4}$$

Then, instead of equating the left-hand sides of (7.2) and (7.3), one gets the relation

$$\frac{1}{\pi M^2}\int e^{-s/M^2}\sigma(s)\,ds = \hat{C}_1\langle 1\rangle + \hat{C}_2\frac{m\langle\bar{q}q\rangle}{2!M^4} + \frac{\hat{C}_2'}{2!M^4}\langle F\cdot F\rangle + \cdots \frac{h_n}{n!M^{2n}} + \cdots . \tag{7.5}$$

This trick provides a double miracle: the right-hand side converges much faster for moderate M^2, and the integral on the left-hand side is rapidly damped for $s > M^2$. Therefore if we choose, for example, $M^2 = m_\rho^2$, we can safely saturate the integral for the I = 1 part of the vector current with the ρ-meson contribution. The coefficient functions $\hat{C}_i$ in (7.5) are related to the C_i in (7.3) by

$$\hat{C}_i(\ln M^2) = C_i(\ln M^2)\left[1 + O\left(\frac{1}{\ln M^2}\right)\right] \tag{7.6}$$

and are calculated in the QCD leading log approximation. Some assumptions have to be made in evaluating the vacuum expectation values appearing in (7.5). The quantity $m\langle\bar{q}q\rangle$ is determined by standard soft-pion techniques

$$(m_u + m_d)\langle\bar{u}u + \bar{d}d\rangle \simeq -f_\pi^2 m_\pi^2 \tag{7.7}$$

$\langle F\cdot F\rangle$ can be evaluated for the presumably dominant one-instanton configuration, but the size integration diverges. The authors prefer to determine $\langle F\cdot F\rangle$ from their analogous sum rules for the charmonium states; the result corresponds to an instanton size cut-off $\rho < (200\ \text{MeV})^{-1}$, which seems plausible. They also find a non-negligible contribution from the four-quark operator, which they approximate by

$$\langle(\bar{q}q)(\bar{q}q)\rangle \simeq |\langle\bar{q}q\rangle|^2 = m_\pi^4 f_\pi^4/m_q^2\ , \tag{7.8}$$

and which can become large if the quark masses are very small. Using values of α_s and m_q which they justify on the basis of other calculations, they find [neglecting corrections O(1%)]

$$m_\rho^2 \simeq 0.6\ \text{GeV}\ ,\quad g_\rho^2/4\pi \simeq 2.42\ ,$$

in excellent agreement with the experimental values

$$m_\rho^2 = 0.602\ ,\quad g_\rho^2/4\pi = 2.36 \pm 0.18\ .$$

Equally remarkable results are obtained by considering currents with different quantum numbers, pseudoscalar densities, etc.

However, the results appear to depend strongly on the choice of the parameters α_s and m_q, which are taken smaller than the values accepted by most theorists. For example, their value of α_s is the one extracted from lowest-order QCD charmonium analysis, which has been found to suffer large higher-order corrections[61], rather than the higher values extracted from deep inelastic scattering data. In addition, the validity of their results depends on the $O(Q^{-12})$ non-perturbative corrections being negligible at the ρ mass. The effective scale parameter which was given as 1 GeV in Eq. (5.7) depends explicitly on m_q and α_s, and with the authors' undoubtedly controversial choice it is indeed $< m_\rho$. In spite of these caveats, it would seem difficult to ignore the success their analysis has met with.

Acknowledgements

I have enjoyed many instructive discussions with Rod Crewther, Sidney Coleman, John Ellis, Ronald Horgan, Vojtek Zakrzewski and especially Chris Sachrajda. The writing of this talk was completed at Fermilab, and it is a pleasure to thank Chris Quigg and the theory group for their hospitality. I am indebted to the scientific secretaries Ikaros Bigi and François Martin for invaluable help in preparing the manuscript.

REFERENCES

1) See: H.D. Politzer, Phys. Reports C14, 129 (1974).
A. Peterman (to be published in Phys. Reports).

2) K.G. Wilson, Phys. Rev. 179, 1499 (1969).
B.L. Ioffe, Phys. Lett. 30B, 123 (1969).
R.A. Brandt and G. Preparata, Nucl. Phys. B27, 541 (1971).
Y. Frishman, Ann. Phys. (NY) 66, 373 (1971).

3) E.C.G. Stueckelberg and A. Peterman, Helv. Phys. Acta 26, 499 (1953).
M. Gell-Mann and F. Low, Phys. Rev. 95, 1300 (1954).

4) C.H. Llewellyn Smith, Proc. 17th Int. Universitätswochen für Kernphysik, Schladming, 1978 [Acta Phys. Austriaca, Suppl. XIX, 331 (1978)].
K.H. Craig and C.H. Llewellyn Smith, Phys. Lett. 72B, 349 (1978).
Yu.L. Dokshitzer, D.I. D'yakanov and S.I. Troyan, Material for the 13th Leningrad Winter School, 1978 [SLAC TRANS-183 (1978)].
D. Amati, R. Petronzio and G. Veneziano, Nucl. Phys. B140, 54 (1978) and B146, 29 (1978).
For earlier related developments see, for example:
S.J. Chang and P.M. Fishbane, Phys. Rev. D 2, 1084 (1970).
V.N. Gribov and L.N. Lipatov, Sov. J. Phys. 15, 438 (1972).
I. Halliday, Nucl. Phys. B103, 343 (1976).
J. Frenkel, M.J. Shailer and J.C. Taylor, Nucl. Phys. B148, 228 (1979).
I. Hinchliffe and C.H. Llewellyn Smith, Phys. Lett. 65B, 281 (1971).
J.L. Cardy and G.B. Winbow, Phys. Lett. 52B, 95 (1974).

5) A partial list of references is:
R.F. Cahalan, K.A. Geer, J. Kogut and L. Susskind, Phys. Rev. D 11, 1199 (1975)
J. Ellis, M.K. Gaillard and G.G. Ross, Nucl. Phys. B111, 253 (1976).
T.A. De Grand, Y.J. Ng and S.-H. Tye, Phys. Rev. D 16, 325 (1977).
E.G. Floratos, Nuovo Cimento 43A, 241 (1977).
H.D. Politzer, Phys. Lett. 70B, 430 (1977).
R. Cutler and D. Sivers, Phys. Rev. D 16, 679 (1977).
B. Combridge, J. Kripfganz and J. Ranft, Phys. Lett. 70B, 234 (1977).
A.P. Contogouris, R. Gaskell and S. Papadopoulos, Phys. Rev. D 17, 2314 (1978).

6) A.A. Belavin, A.M. Polyakov, A.S. Schwarz and Yu.S. Tyupkin, Phys. Lett. 54B, 856 (1975).

7) N. Cabibbo and L. Maiani, Phys. Lett. 79B, 109 (1978).
M. Suzuki, LBL preprint 7948 (1978).
N. Cabibbo, G. Corbo and L. Maiani, Rome Univ. preprint ROM 79-145 (1979).
A. Ali and A. Pietarinen, DESY preprint 79/12 (1979).
See also M.K. Gaillard, Proc. SLAC Summer Inst. on Particle Physics, Stanford, 1978 (SLAC Report No. 215, 1978), p. 397.

8) A. Billoire, R. Lacaze, A. Morel and H. Navelet, Phys. Lett. 78B, 140 (1978); and Saclay preprint DPh-T/78/111 (1978).
W. Bernreuther, N. Marinescu and M.G. Schmidt, Heidelberg preprint HD-THEP-79-5 (1979).

9) G.P. Lepage and S.J. Brodsky, SLAC preprints SLAC-PUB-2348 and 2343 (1979).
For earlier work, see R. Coquereaux and E. de Rafael, Phys. Lett. 74B, 105 (1978).

10) E.G. Floratos, D.A. Ross and C.T. Sachrajda, Nucl. Phys. B129, 66 (1977) and B139, 545 (1978).
W.A. Bardeen, A.J. Buras, D.W. Duke, and T. Muta, Phys. Rev. D 18, 3998 (1978).

11) O. Nachtmann, Nucl. Phys. B63, 239 (1973) and B78, 455 (1974).

12) J. Kogut and L. Susskind, Phys. Rev. D 9, 697 (1974) and D 9, 3391 (1974).

13) G. Altarelli and G. Parisi, Nucl. Phys. B126, 298 (1977).

14) L. Baulieu and F.C. Kounnas, Paris preprint LPTENS 78/27 (1978).

15) I follow closely the descriptions given by C.H. Llewellyn Smith, Ref. 4, and C.T. Sachrajda, Proc. 10th GIFT Seminar on Theoretical Physics (1979), in preparation.

16) H.D. Politzer, Nucl. Phys. B129, 301 (1977).
C.T. Sachrajda, Phys. Letters 73B, 185 (1978).
C.T. Sachrajda, Phys. Letters 76B, 100 (1978).

17) B. Humpert and W.L. Van Neerven, COO-881-54/ Rev. (1978), Phys. Lett. B, to be published.
G. Altarelli, K. Ellis and G. Martinelli, MIT preprint, MIT-77619 (1979).
K. Harada, T. Kanako and N. Sakai, CERN preprint TH-2619 (1979).

18) R.K. Ellis, H. Georgi, M. Machacek, H.D. Politzer and G.G. Ross, Nucl. Phys. B152, 285 (1979).
S. Libby and G. Sterman, Phys. Rev. D 17, 2773 and 2789 (1978).

19) G. Sterman and S. Weinberg, Phys. Rev. Lett. 39, 1436 (1977).
See also:
B.G. Weeks, Phys. Lett. 81B, 377 (1979).
K. Shizuya and S.-H. Tye, Phys. Rev. Lett. 41, 787 and 1195(E) (1978).
M.B. Einhorn and B. Weeks, SLAC-PUB-2164 (1978).

20) P. Binétruy and G. Girardi, Phys. Lett. 83B, 339 (1979).

21) Data: Ch. Berger et al., PLUTO Collaboration, Phys. Lett. 82B, 449 (1979).
Calculation: I.I.Y. Bigi and T.F. Walsh, Phys. Lett. 82B, 267 (1979).

22) S. Brandt, Ch. Peyrou, R. Sosnowski and A. Wroblewski, Phys. Lett. 12, 57 (1964).
E. Farhi, Phys. Rev. Lett. 35, 1609 (1975).

23) H. Georgi and M. Macharek, Phys. Rev. Letters 39, 1237 (1977).

24) J.D. Bjorken and S.J. Brodsky, Phys. Rev. Lett. D 1, 1416 (1977).

25) Private communications from experimentalists.

26) S. Brandt and H.D. Dahmen, Z. Phys. C1, 61 (1979).

27) A. De Rújula, J. Ellis, E.G. Floratos and M.K. Gaillard, Nucl. Phys. B138, 387 (1978).

28) PLUTO Collaboration, see H. Meyer, *in* Highly Specialized Seminars, Erice, 1979.

29) Ch. Berger et al., PLUTO Collaboration, Phys. Lett. 78B, 176 (1978).

30) K. Koller, H. Krasemann and T.F. Walsh, Z. Phys. C1, 71 (1979).

31) G. Fox and S. Wolfram, Phys. Lett. 82B, 134 (1979); Phys. Rev. Lett. 41, 1581 (1979); and Nucl. Phys. B149, 413 (1979).
J.F. Donoghue, F.E. Low and S.Y. Pi, MIT preprint, MIT-CTP 771 (1979).

32) K. Koller and T.F. Walsh, Phys. Lett. 72B, 227 (1977) and E 73B, 504 (1978).
G. Parisi, Phys. Lett. 74B, 65 (1978).
C.L. Basham, L.S. Brown, S.D. Ellis and S.T. Love, Phys. Rev. Lett. 41, 1585 (1978), Phys. Rev. D 17, 2298 (1978), and Univ. of Washington preprint RLO-1388-759 (1978).
G. Parisi and R. Petronzio, Phys. Lett. 82B, 26 (1979).
E.G. Floratos, Saclay preprint DPh T/79/89 (1979).

33) H. Fritzsch and K.H. Streng, Phys. Lett. 74B, 90 (1978).
S.-Y. Pi, R.L. Jaffe and F.E. Low, Phys. Rev. Lett. 41, 142 (1978).
S.-Y. Pi and R.L. Jaffe, MIT preprint CPT 735 (1978), to appear in Phys. Rev. D Comments and Addenda.
J. Ellis and I. Karliner, Nucl. Phys. B148, 141 (1979).

34) M. Krammer and H. Krasemann, Phys. Lett. 73B, 58 (1978).
H. Krasemann, Z. Phys. C1, 189 (1979).

35) H. Georgi and H.D. Politzer, Phys. Rev. Lett. 40, 3 (1978).
G. Ranft and J. Ranft, Leipzig Univ. preprint 78-15 (1978).
A. Méndez, Nucl. Phys. B145, 199 (1978).
A. Méndez, A. Raychaudhuri and V.J. Stenger, Nucl. Phys. B148, 499 (1979).
J. Cleymans, Phys. Rev. D 18, 954 (1978).
G. Köpp, R. Maciejko and P.M. Zerwas, Nucl. Phys. B144, 123 (1978).
G. Altarelli and G. Martinelli, Phys. Lett. 76B, 89 (1978).
P. Mazzanti, R. Odorico and V. Roberto, Bologna preprint IFUB/78-11 (1978).
F. Hayot and A. Morel, Saclay preprint DPh-T/79/3 (1979).
K.H. Streng, T.F. Walsh and P.M. Zerwas, DESY preprint 79/10 (1979).

36) P. Binétruy and G. Girardi, CERN preprint TH-2611 (1979) to be published in Nucl. Phys. and *in* Highly Specialized Seminars, Erice, 1979.

37) J.B. Kogut, Phys. Lett. 65B, 377 (1976).
D. Lopez, Phys. Rev. Lett. 38, 461 (1977).
A.V. Radyshkin, Phys. Lett. 69B, 245 (1977).
J. Kogut and J. Shigimitsu, Nucl. Phys. B129, 461 (1977).
H. Fritzsch and P. Minkowski, Phys. Lett. 73B, 80 (1978).
G. Altarelli, G. Parisi and R. Petronzio, Phys. Lett. 76B, 351 and 356 (1978).
K. Kajantie and R. Raitio, Helsinki preprint HU-TFT 77-21 (1977).
F. Halzen and D. Scott, Phys. Lett. 79B, 123 (1978).
K. Kajantie and J. Lindfors, Helsinki preprint ISBN 951-45-1487-4 (1978).

38) H. Fritzsch and P. Minkowski, Phys. Lett. 69B, 316 (1977).
Z. Kunszt and E. Pietarinen, DESY preprint 79/18 (1979).
Z. Kunszt, E. Pietarinen and E. Reya, DESY preprint DESY 79/28 (1979).

39) R. Horgan, private communication.

40) E. Witten, Nucl. Phys. B120, 189 (1977).

41) C.H. Llewellyn Smith, Phys. Lett. 79B, 83 (1978).
W.R. Frazer and J.F. Gunion, Phys. Rev. D 19, 2447 (1979).

42) S.J. Brodsky, T.A. Debrand, J.F. Gunion and J.H. Weis, Phys. Rev. D 19, 1418 (1979).

43) Tu Tung-Sheng and Wu Chi-Min, CERN preprint TH-2646 (1979).
Chang Chao-Hsi, Tu Tung-Sheng and Wu Chi-Min, CERN preprint TH-2675 (1979).

44) G.R. Farrar and B.L. Ioffe, Phys. Letters 71B, 118 (1977).
K. Koller, T.F. Walsh and P.M. Zerwas, DESY preprint 78/77 (1978).

45) M. Abud, R. Gatto and C.A. Savoy, Univ. of Geneva preprint UGVA-DPT 1979/03-192 (1979).

46) C.H. Llewellyn Smith, *in* LEP Summer Study, Les Houches, 1978 (CERN 79-01, 1979), p. 35.

47) G. 't Hooft, Phys. Rev. Lett. 37, 8 (1976); Phys. Rev. D 14, 3432 (1976) and Erratum in D18, 2199 (1978).
C.G. Callan, R. Dashen and A.J. Gross, Phys. Lett. 63B, 334 (1976) and 66B, 375 (1977).

48) N. Andrei and D.J. Gross, Phys. Rev. D 18, 468 (1978).
L. Baulieu, J. Ellis, M.K. Gaillard and W.J. Zakrzewski, Phys. Lett. 77B, 290 (1978).
T. Appelquist and R. Shankar, Phys. Lett. 78B, 468 (1978).

49) L.S. Brown, R.D. Carlitz, D.B. Creamer and C. Lee, Phys. Lett. 70B, 180 (1977).

50) L. Baulieu, J. Ellis, M.K. Gaillard and W.J. Zakrzewski, Phys. Lett. 81B, 41 (1979).
C.A. Flory, LBL preprint 8499 (1979).

51) J. Ellis, M.K. Gallard and W.J. Zakrzewski, Phys. Lett. 81B, 224 (1979).

52) C.G. Callan, R. Dashen and D.J. Gross, Phys. Rev. D17, 2717 (1978).
F. Wilczek and A. Zee, Phys. Rev. Lett. 40, 83 (1978).
C.G. Callan, R. Dashen, D.J. Gross, F. Wilczek and A. Zee, Phys. Rev. 18, 4684 (1978).
W. Bernreuther et al., Ref. 8.

53) See, however, Appelquist and Shankar, Ref. 48.

54) S.L. Glashow, *in* Hadrons and their interactions (Academic Press Inc., New York, 1968), p. 83.
S. Weinberg, Phys. Rev. D 11, 3583 (1975).

55) J. Kogut and L. Susskind, Phys. Rev. D 11, 3594 (1975).

56) G. 't Hooft, Ref. 47.

57) R.J. Crewther, Phys. Lett. 70B, 349 (1977).

58) R.J. Crewther, Riv. Nuovo Cimento 2, No. 8 (1979) p. 63.

59) H. Goldberg, Northwestern University preprint NUB No. 2397 (1979).

60) M.A. Shifman, A.I. Vainshtein and V.I. Zakharov, Nucl. Phys. B147, 385, 448 and 519 (1979).

61) R. Barbieri, E. d'Emilio, G. Curci and E. Remiddi, CERN preprint TH-2622 (1979).